

## Arrested cracks in nonlinear lattice models of brittle fracture

David A. Kessler\*

*Department of Mathematics, Lawrence Berkeley National Laboratory, 1 Cyclotron Road, Berkeley, California 94720*

Herbert Levine

*Department of Physics, University of California, San Diego, La Jolla, California 92093-0319*

(Received 22 January 1999)

We generalize lattice models of brittle fracture to arbitrary nonlinear force laws and study the existence of arrested semi-infinite cracks. Unlike what is seen in the discontinuous case studied to date, the range in driving displacement for which these arrested cracks exist is very small. Also, our results indicate that small changes in the vicinity of the crack tip can have an extremely large effect on arrested cracks. Finally, we briefly discuss the possible relevance of our findings to recent experiments. [S1063-651X(99)10212-5]

PACS number(s): 62.20.Mk, 46.50.+a

Recent years have seen a rebirth of interest among the physics community in the issue of dynamic fracture. This is due to a variety of new experimental results which are not explainable within the confines of the traditional engineering approach to fracture [1]. These results include a dynamical instability to microbranching [2,3], the formation of non-smooth fracture surfaces [4], and the rapid variation of the fracture energy (including dissipative losses incurred during cleavage) with crack velocity [5]. These issues are reviewed in a recent paper by Fineberg and Marder [6]. This renewed interest serves as motivation for us to introduce a new class of lattice models for fracture; eventually, we hope that the tractability of our models, as shown below for the simpler problem of lattice pinning, will lead to insight into all of these issues.

One approach for dealing with dynamic fracture involves restricting the atomic interactions to those occurring between neighboring sites of an originally unstrained lattice. These lattice models can never be as realistic as full molecular-dynamics simulations, but compensate for this shortcoming by being much more amenable to analysis, both numerical and (via the Wiener-Hopf technique) otherwise. This approach was pioneered by Slepyan and co-workers [7] and further developed by Marder and Gross [8] and most recently by us [9]. Most of the results to date have been obtained using a simplified force law which is linear until some threshold displacement, at which point it drops abruptly to zero. Below, we will study a generalization for which the force is a smooth function of the lattice strain. One of our goals is to learn which aspects of fracture are sensitive to microscopic details and which are universal.

One interesting aspect of these lattice models concerns the existence of a range of driving displacements  $\Delta$  for which nonmoving semi-infinite crack solutions can be found. For the aforementioned discontinuous force model, there exists a wide range of these arrested cracks. For example, Ref. [9] found that  $\Delta$  could range from 40% below to 40% above the Griffith displacement  $\Delta_G$ , the driving at which it first be-

comes energetically favorable for the system to crack. This phenomenon is connected to the existence of a velocity gap, i.e., a minimal velocity for stable crack propagation. Experimentally, no such gap has been reported, even for materials such as single-crystal silicon [10], which should be at least approximately describable by lattice models. It is therefore of some interest to study how the arrested crack range depends on the microscopic details of the assumed atomic force law. Here we present the results of such a study, including the finding that this range drops rapidly towards zero as the force law is made smoother and hence more realistic.

As in Ref. [9], we work with a square lattice and with scalar displacements (mode III). We focus on arrested cracks and write the static equation as

$$0 = -f(u_{i+1,j} - u_{i,j}) + f(u_{i,j} - u_{i-1,j}) - f(u_{i,j+1} - u_{i,j}) + f(u_{i,j} - u_{i,j-1}). \quad (1)$$

Here the indices  $\{i,j\}$  label the lattice site and  $u$  is the displacement. Sites in the last row of the lattice,  $j=N_y$ , are coupled to a row with fixed displacement  $\Delta$ . The first row,  $j=1$ , is coupled to a  $j=0$  displacement field  $u_{i,0}$  which via symmetry equals  $-u_{i,1}$ . Finally,  $f$  is a nonlinear function of its argument, the lattice strain. We investigate two forms [11]:

$$f_e(u) = -u \frac{1 + \tanh[\alpha(1-u)]}{1 + \tanh \alpha}, \quad (2)$$

$$f_p(u) = -\frac{u\alpha^{\alpha+1}}{(u+\alpha)^{\alpha+1}}. \quad (3)$$

For both of these forms, increasing  $\alpha$  reduces the length scale over which  $f$  falls to zero once outside Hooke's law regime ( $u < 1$ ). The exponential force  $f_e$  reduces to the familiar discontinuous force (linear until complete failure) as  $\alpha \rightarrow \infty$ .

Our procedure for finding solutions is in principle straightforward. At large positive  $i$  in the uncracked material, we know that the system will adopt a uniformly strained state. Conversely, at large negative  $i$  the cracked state will

\*Permanent address: Dept. of Physics, Bar-Ilan University, Ramat Gan, Israel.

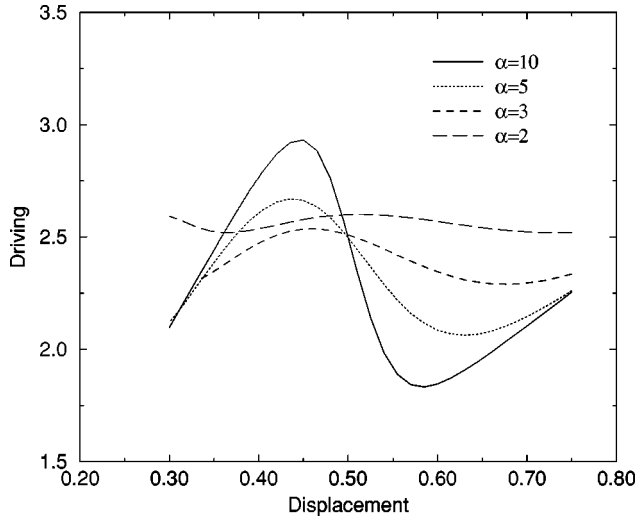


FIG. 1.  $\Delta$  vs imposed  $u_{0,1}$  (dimensionless) displacement for different values of  $\alpha$  in  $f_e$ . All data have  $N_y=10$  and  $N_x=100$ .

have a large displacement  $u_{i,1}$  and (almost) zero strains for  $j>1$ . Fixing the boundary condition  $\Delta$  allows us to easily find these asymptotic states. Once found, these solutions are used as fixed displacements for the columns  $i=N_x+1$  and  $i=-N_x-1$ , respectively. The arrested crack then requires us to solve for  $(2N_x+1)N_y$  variables. We impose the equation at motion at all sites except for the crack “tip” ( $i=0, j=1$ ), where instead we specify the displacement; this approach preserves the banded structure of the system. Newton’s algorithm then allows us to converge to a solution. Afterwards, the residual equation of motion becomes a solvability condition with which  $\Delta$  can be determined. The range of allowed values of  $\Delta$  for arrested cracks is found as one systematically sweeps through the value of the aforementioned fixed displacement.

In Fig. 1 we present our results for the exponential model. For illustration, we have chosen to show data for  $N_y=10$  as a function of  $\alpha$ . For large  $\alpha$ , the range of  $\Delta$  is large and there is a marked asymmetry between the rising segment of  $\Delta$  versus imposed displacement and the (much steeper) falling segment. As  $\alpha \rightarrow \infty$ , the falling portion becomes vertical. These segments represent different crack solutions at fixed  $\Delta$ ; as  $\Delta$  reaches the end of its allowed range, these solution branches collide and disappear in a standard saddle-node bifurcation point. To verify this, we have performed [12] a linear stability calculation of these solutions, assuming purely inertial dynamics [i.e., setting the left-hand side of Eq. (1) to  $\ddot{u}_{i,j}$ ]. As expected, there is a single mode of the spectrum for the growth rate  $\omega$  for which  $\omega^2$  goes from negative to positive as we go up the rising segment, reach the maximal driving, and then go back down.

Figure 1 demonstrates that as the potential is made smoother, the range of arrested cracks shrinks dramatically. In Fig. 2, we show this range as a percentage of  $\Delta_G$ . The best fit to our data suggests that the range vanishes as an essentially singular function of  $\alpha$ ,

$$\frac{\Delta_{\max} - \Delta_{\min}}{\Delta_G} \sim A \exp\left(-\frac{\alpha_0}{\alpha}\right), \quad (4)$$

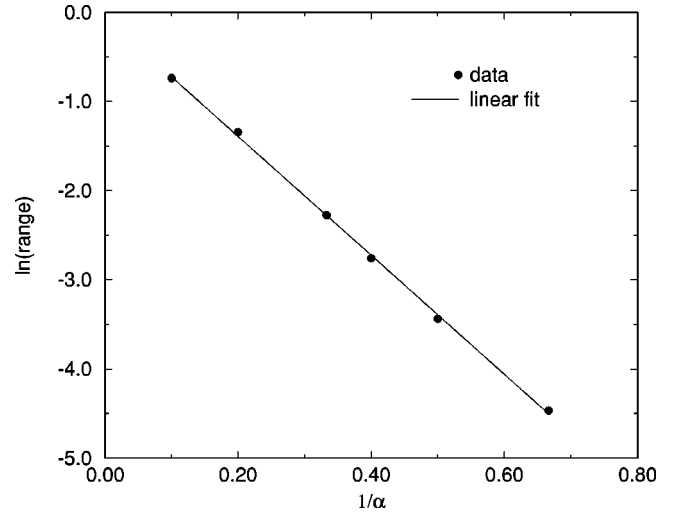


FIG. 2. Arrested crack range normalized by the Griffith displacement  $\Delta_G$  vs  $\alpha$  in  $f_e$ ; again all data are for  $N_y=10$ ,  $N_x=100$ .

where for  $N_y=10$ ,  $\alpha_0 \approx 6.6$  and otherwise is a slowly varying function of  $N_y$  as long as the system is sufficiently large compared to the potential fall-off.

Let us now turn to the power-law form. Based on our findings above, we would expect that this rather smooth force law would give rise to a range which is practically zero. We have verified this prediction in two ways. First, for the case  $\alpha=3$  we performed our usual scan over imposed  $u_{0,1}$  displacement and noted that the selected  $\Delta$  varies by less than  $10^{-6}$ . Second, we computed the stability spectrum and found a mode at  $\omega^2 < 10^{-6}$ ; this value is indicative of how close we are at a randomly chosen displacement to the extremal value of  $\Delta$  at the saddle-node bifurcation. These numbers are consistent with our numerical accuracy and hence the true range is probably even smaller. Needless to say, ranges of this size would be unmeasurable. It is interesting to point out that the almost-zero mode is nothing other

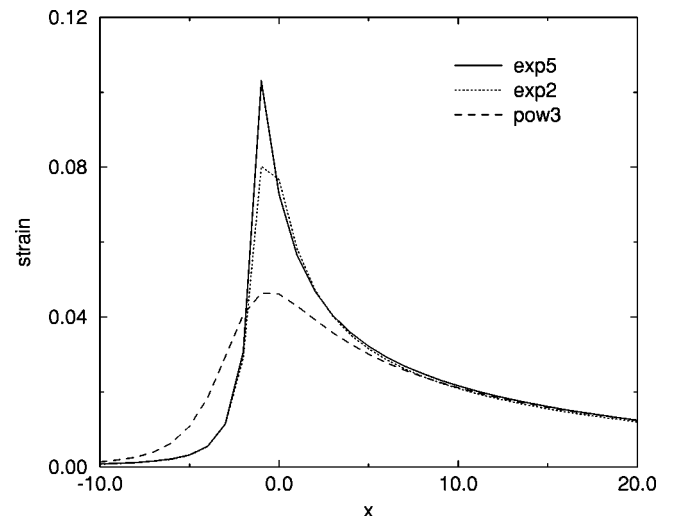


FIG. 3. Dimensionless strain  $u_{i+1,1} - u_{i,1}$  for three different potentials. Data are for  $N_y=40$ ,  $N_x=200$  and are normalized to the respective  $\Delta$  values. The power-law curve has been shifted two sites to the left so as to better match the field at large positive  $i$ .

than a spatial translation of the crack. That is, translating the crack with respect to the underlying fixed lattice is almost a symmetry of the solution.

So, by making the potential smoother one tends to eliminate arrested crack solutions. How does this change come about? To try to address this question, we plot in Fig. 3 the lattice strain field  $u_{i+1,1} - u_{i,1}$  for  $-N_x \leq i \leq N_x$  for the three potentials, exponential with  $\alpha=5$  (exp 5) or 2 (exp 2) and power-law with  $\alpha=3$  (pow 3). For this comparison, we have found (stable) solutions with  $u_{0,1}=0.75$  for all three potentials, and then normalized the strains by dividing with the respective values of  $\Delta$ . First, we note that beyond  $x \approx 5$ , the different cases are virtually indistinguishable and all lie on the expected  $x^{-1/2}$  universal curve [1,9]. The interior “process-zone” region is affected by changing the potential, but rather minimally. For example, the two exponential cases differ in only one or two points, yet this is sufficient to shrink the arrested crack range by almost an order of magnitude. The power-law choice has a process zone which is a bit wider and there is less maximal strain, but that is all. We thus conclude that the existence and size of the arrested crack range are extremely sensitive to microscopic details. We note in passing that the process zone for any specific potential quickly reaches an asymptotic size once  $N_y$  is sufficiently large and in particular does not increase indefinitely in the macroscopic limit. Treatments [13,14] which include a

mesoscopic-size “cohesive-zone” are therefore not accurate representations of this class of lattice models.

In a recent experiment [10] on fracture in silicon, no arrested cracks were observed. A molecular-dynamics simulation using a modified Stillinger-Weber potential also exhibited no arrested cracks when studied at high enough temperature. However, the potentials used here were rather short-ranged, as compared with some estimates that arise from density-functional theory [15]. Our results indicate that increasing the range and thereby using smoother potentials will eliminate (at least as far as experimentally attainable precision occurs) arrested cracks and may offer a simpler explanation of the experimental finding than one which requires thermal creep. This could of course be tested in principle by redoing the experiments at a reduced temperature.

H.L. acknowledges the support of the U.S. NSF under Grant No. DMR98-5735; D.A.K. acknowledges the support of the Israel Science Foundation and the hospitality of the Lawrence Berkeley National Laboratory. The work of D.A.K. was also supported in part by the Office of Energy Research, Office of Computational and Technology Research, Mathematical, Information and Computational Sciences Division, Applied Mathematical Sciences Subprogram, of the U.S. Department of Energy, under Contract No. DE-AC03-76SF00098. Also, D.A.K. acknowledges useful conversations with M. Marder and G. Barenblatt.

- 
- [1] L. B. Freund, *Dynamic Fracture Mechanics* (Cambridge University Press, Cambridge, England, 1990).
- [2] J. Fineberg, S. P. Gross, M. Marder, and H. L. Swinney, *Phys. Rev. Lett.* **67**, 457 (1992); *Phys. Rev. B* **45**, 5146 (1992).
- [3] E. Sharon, S. P. Gross, and J. Fineberg, *Phys. Rev. Lett.* **74**, 5096 (1995).
- [4] J. F. Boudet, S. Ciliberto, and V. Steinberg, *Europhys. Lett.* **30**, 337 (1995).
- [5] E. Sharon, S. P. Gross, and J. Fineberg, *Phys. Rev. Lett.* **76**, 2117 (1996).
- [6] J. Fineberg and M. Marder, *Phys. Rep.* **313**, 2 (1999).
- [7] L. I. Slepyan, *Dokl. Akad. Nauk* **258**, 561 (1981) [*Sov. Phys. Dokl.* **26**, 538 (1981)]; **324**, 69 (1992) [**37**, 259 (1992)]; Sh. A. Kulamekhtova, V. A. Saraikin, and L. I. Slepyan, *Mech. Solids* **19**, 101 (1984).
- [8] M. Marder and S. Gross, *J. Mech. Phys. Solids* **43**, 1 (1995).
- [9] D. Kessler and H. Levine, *Phys. Rev. E* **59**, 5154 (1998).
- [10] J. A. Hauch, D. Holland, M. P. Marder, and H. L. Swinney, *Phys. Rev. Lett.* **82**, 3823 (1999).
- [11] In principle, one might want to take  $f$  for mode III to be explicitly odd with respect to  $u$ . We have opted for defining the forces in Eq. (1) in such a way as to guarantee that all large strains are positive and hence the nonlinear behavior of  $f$  for large negative argument is irrelevant.
- [12] We linearize the equation around the arrested crack solution and determine the eigenvalues  $\omega^2$  directly from the stability matrix of linear size  $(2N_x + 1)N_y$  (assuming that the perturbation maintains the odd symmetry  $u_{i,0} = -u_{i,1}$ ).
- [13] J. S. Langer and A. E. Lobkovsky, *J. Mech. Phys. Solids* **46**, 1521 (1998).
- [14] G. I. Barenblatt, *Adv. Appl. Mech.* **7**, 56 (1962).
- [15] See, for example, H. Rucker and M. Methfessel, *Phys. Rev. B* **52**, 11 059 (1995).